

Quantum Transmission Modelling in Graphene Nano Scrolls (GNSs) of Double Barrier

S.N. Hedayat, M.T. Ahmadi, H. Sedghi, H. Goudarzi

Abstract- Graphene has amazing carrier transport property and high sensitivity at the single molecule level which leads them as a promising material for biosensor application. In order to develop the new device types same as graphene nanoribbon, Carbon Nanotube Field Effect Transistor (CNTFET) and Nanowire, it is essential to investigate of quantum limit in low dimensional devices. In this paper quantum current of double barrier Graphene Nano scroll (DGNS) is modelled and the electronic properties due to the dependence on structural parameter are analyzed. In addition, 1D quantum transport coefficient based on the approximation of the wave vector relation for MGNS is presented.

The present paper deals with quantum transmission on GNS for double barrier and also models current-voltage characteristic based on quantum transport given structural parameters electronic Properties are analyzed. In addition, 1D quantum transport is presented based on the wave vector approximation on GNS.

Index Terms: Quantum transmission, Double barrier, Graphene Nano scrolls, quantum current, energy

I.INTRODUCTION

For first time, Graphene molecules were extracted from a graphite crystal as per a simple micromechanical approach [1,2]. In process of peeling out of graphite crystal, mechanical stress exertion causes segregates graphene layers, in turn contrasting the interlayer interaction forces. This approach is so called Scotch type or drawing method as the mechanical exfoliation is the same as writing with a pencil. Foregoing approach enable graphene production in sufficient quantities to evaluate fundamental physics. Since its initial discovery, there have been wide varieties of experimental approaches and chemical synthesis methods to achieve graphene sheets so that they can be promising to fabricate enormous tools and materials to be applied in specific technological applications. Significant deviation undergone by the graphene sheets from planar geometry has received great deal of attentions [3].

S.N. Hedayat, Department of physic, Faculty of science, Urmia University, Urmia, Iran

M.T. Ahmadi, Department of physic, Faculty of science, Urmia University, Urmia, Iran

H. Sedghi, Department of physic, Faculty of science, Urmia University, Urmia, Iran

H. Goudarzi, Department of physic, Faculty of science, Urmia University, Urmia, Iran

due to formation of some ripples with local curvature, membranes, ribbons, as well as structures, many questions have been a Rosen both from the theoretical and the practical view points, including what are the controlling parameters and what role they play in determining the conformational changes in a low-dimensional material including graphene, and to which extent it is possible to control the occurrence of these morphological variations to meet a goals. producing and assembling high-quality structures for large-scale graphene applications. Scrolled graphene sheets are very substantial carbon nanostructures having wide verities of promising physical characteristics (e.g., very high specific surface area, and electrical as well as thermal conductivity), suitable for enormous applications in different technological fields like, for example, sorbents, catalyst supports, highly porous electrodes for batteries and super capacitors, hydrogen storage materials, fillers for high-strength structural composites, etc. [4,5].

As a key material Graphene-based material have been put forwarded in nanotechnology and frequently have been considered in various applications. Reduced graphene oxide (RGOx) Nano scrolls serve as a new member belonged to graphene family, made by rolling single graphene sheets from opposite side or from a corner to form Archimedean-type spirals, more commonly so called Swiss rolls. graphene Nano scrolls thanks to their unique structure, presumably have excellent high conductance of single graphene sheets. The opposite is true for single-walled carbon nanotubes in which contingent upon their diameter and chirality some structural constraints on the electron wave functions make them either metallic or semiconducting. Simultaneously with unique electronic properties, there is an appropriate layer spacing of Nano scrolls allowing for energy storage applications. there are consensuses that the graphene based materials are characterized with better electrical transmission. Electronic devices production in tremendously small dimensions (fewer than 100 nanometers) may be attributed to modern advances in production of atomic-sized conductors. Until now, wide varieties of literatures on CNT and GNR have been reported [6, 7]. Indeed, graphene Nano scrolls are found to be small graphene nanoribbon scrolled up into the spiral [8, 9]. The GNS formation mechanisms are greatly similar to mechanisms in relation to characteristic large graphene and boron nitride Nano scrolls. The rolled layers overlapping surface in GNSs improves structural stability [10]. Graphene Nano scrolls are protective materials to generate Nano

electronic devices, as channel and interconnection in FETs and MOSFETs [11, 12]. While outlining Nano scrolls structure, the electron microscopy and diffraction have been introduced as very efficient approaches [13, 14]. GNSs can be used as electron-transport carrier [15, 16]. Now a day, the quasi-one-dimensional Nano carbons, i.e., the Nano wall, nanowire, Nano belt, and Nano scroll, is synthesized according to hydrothermal method or the plasma enhanced chemical vapor deposition (CVD) [17, 18, 19]. A simple and efficient method for constructing the high-quality carbon Nano scrolls (CNSs) is found to be apply isotropy alcohol solution to rolling up the monolayer graphene predefined on substrates has been considered as. In addition, it is proved that the GNS has great importance and this method would be capable of sustaining a high current density. This in turn suggests that it can be taken as a proper occurs alternative for microcircuit inter connects [20, 21].

Graphene Nano scroll (GNS) with spiral structure is featured as a rolled up Graphene with one dimensional structure as it is illustrated in figure (1) [26, 27]. a simple fabrication method to GNS production has been proposed wet chemistry technique [28, 29] as well as hydrogenation on one side it can be scroll up completely into a graphene Nano scroll (GNS) which is stable over room temperature [30, 31].

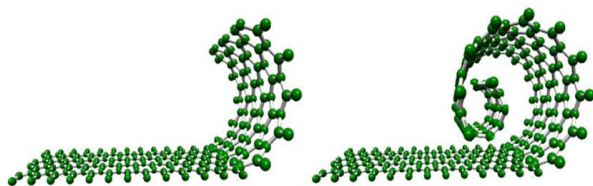


Figure (1): Graphene Nan scroll geometries

Given the Raman characteristics of Nano scrolls, new bands, G-peak and D-peak in the low-wave number area have been evaluated [32]. Also there have been literature on GNS transport properties upon uniform electric field [33]. Graphene Nano scrolls due to its unique electronic and physical properties including high carrier mobility, unconventional quantum Hall effect together with potential applications in Nano electronics had led to they considered as main attractive subjects [34,36]. At the same time their possible application relates to high speed switching devices [35]. Furthermore, at unable band gap on graphene Nano scrolls(GNS) leads to the field-effect transistors (FET) applications. [37,38].

There have been completed theoretical descriptions on electron transport in a bridge system of GNS as well as fundamental mechanisms underlying the electron transport in bridge systems. In addition, experimental data on electron transport implied as chasm between the theory and practice. Some controlling parameters including geometry of the conducting channel between the two electrodes, the coupling of bridging material, current amplitude and quantum interference effect have been considered. Moreover, the dynamical instability in the Nano -scale devices may control

electron transport as well. However, there has been a little information about the role of quantum effects in GNS MOSFET. The present paper deals with quantum transmission on GNS and also models current-voltage characteristic based on quantum transport given structural parameters electronic Properties are analyzed. In addition, 1D quantum transport is presented based on the wave vector approximation on GNS.

Also recent studies on pressure sensitivity of the equilibrium core size of CNSs showed some applications of them in Nano pumps, Nano oscillators with high breathing oscillating frequency as well as linear Nano actuators. [40] Such wide range of applications has motivated researchers toward more investigations on CNSs in recent years. CNSs unique electrical properties and their capability of supporting high current density make CNSs an excellent occurs alternative for microcircuit interconnects. An

Analytic model for liquid-gated transistors of CNSs has been reported [41] improving facilitation of device scaling and fabrication using CNSs. According to comparison with CNT devices, CNS transistors exhibits identical behavior as CNT in which CNS also illustrates some superior properties from both graphene and CNT, including high carrier mobility and high mechanical stress. The electronic structures of CNSs are considerably correlated to chirality (n, m) which has been defined in figure (2). there are three enormous types of CNS structures similar to CNT; armchair, zigzag and chiral (helical) CNSs. Armchair CNSs are metallic or semi metallic dependent upon their size and it has been proved that the metallic one have own larger density of states at the Fermi level than metallic single-walled nanotubes (SWNTs). Zigzag CNSs are semiconductors which have much smaller energy gap than similar zigzag SWNTs [39, 42, 43, and 44]. Recent analysis on electrical properties have only been applied on armchair and zigzag CNSs for their convenient modeling [24, 25], but the electrical Properties of a chiral (helical) CNS are still unknown. It has been shown in Figure (2), armchair and zigzag CNSs geometries.

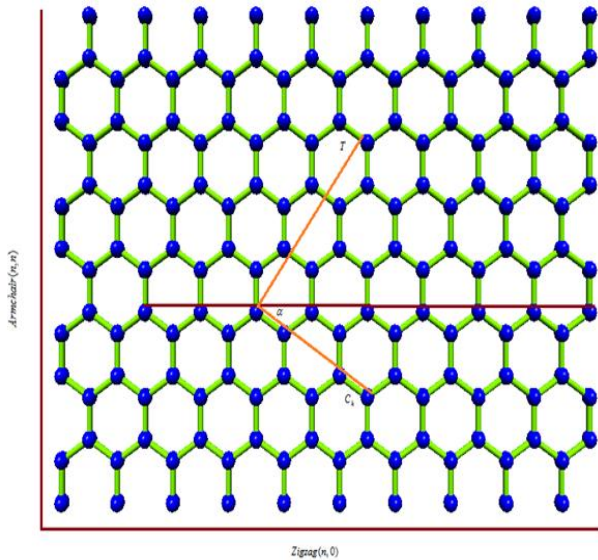


Figure (2): Armchair and zigzag geometries

Molecular Dynamic simulations (MDS) have been supported by CNS fabrication. Also MDS similar to theoretical models illustrates a stable forming of CNS with lower energy than graphene [22, 23]. The scrolling procedure is along with two considerable energy contributions, the elastic energy (influenced by bending the layer) and the free energy (generated by the van der Waals interaction). Increase in the elastic energy and the structure tends to return to its planner configuration while the structure is rolled and before layer overlaps each other. However, by overlapping the rolled layers after a critical diameter value, the van der Waals energy increases and a high stability scrolled structure is formed.

Since a CNS can be considered as a rolled up graphene sheet into a spiral form, band structure of graphene forms the basis of all types of CNSs and so the two dimensional dispersion relation of grapheme can be determined using the tight-binding approximation(TB) which is given by equation (1).

$$(1)$$

Where the positive and negative signs indicate conduction and valence bands respectively, $t = 3\text{eV}$ is the

nearest-neighbor C-C bonding energy, k denotes on wave vector ($k = kx\hat{i} + kj\hat{j}$) and $a_{cc} = 1.42\text{\AA}$ is the nearest neighbor C-C bonding distance.

As carrier transporting through these sorts of devices is anisotropic phenomenon so it provides ease of fabrication of electronic circuits for example ignoring any etching or cutting step. Computing transmission coefficient in an analytical expression for different potential barriers are in our scope of interest, however, it can be calculated by different methods such as S-matrix which is one of the most appropriate techniques for multiple barrier conditions.

As shown in figure (3) in the proposed structure with two semiconducting channel is modulated and connected to drain

and source terminal by three metallic graphene which make a schottcky twin barrier and through the source and drain at the graphene-metal interface in a transistor

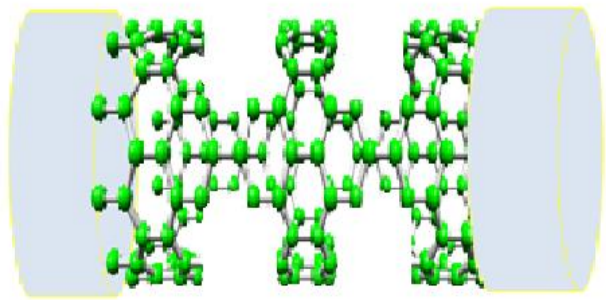


Figure (3): Schematic of three metallic graphene, connecting three pieces of GNS by two bridge semiconductors which each coupled make a schottcky Twin barrier

II. MODELING

In regions 1, 2, 3, 4 and 5, an answer to Schrödinger's equation everywhere $E < V_0$ is of the same shape including traveling and reflecting wave. In regions 1, 3 and 5 the potential energy is estimated to be zero, and in regions 2 and 4 the potential energy is V_0 therefore,

$$k_1 = k_3 = k_5 = \sqrt{\frac{2mE}{\hbar^2}}, k_2 = k_4 = \sqrt{(E - E_g) \frac{2}{3ta_{cc}}} \quad (2)$$

The transmission ratio differs in terms of probability of currents according to T equation

$$T = \left| \frac{j_{transmitted}}{j_{incident}} \right| = \left| \frac{K}{A} \right|^2 \quad (3)$$

To precede our calculations; reflection and transmission amplitudes on junctions are required. Individual barrier does not depend on reflection amplitude. Let R be the reflection amplitude for a hydroplane gesture of component amplitude with energy $E < V_0$ interrupting on a barrier of length L as of the left at $x = 0$, perceive figure (4). T allows the transmission beam to be the same amplitude. Communication, which is recognized by the reflection and transmission facilities, as well as the reflection and transmission coefficients, is therefore $|R|^2$ and $|T|^2$ respectively.

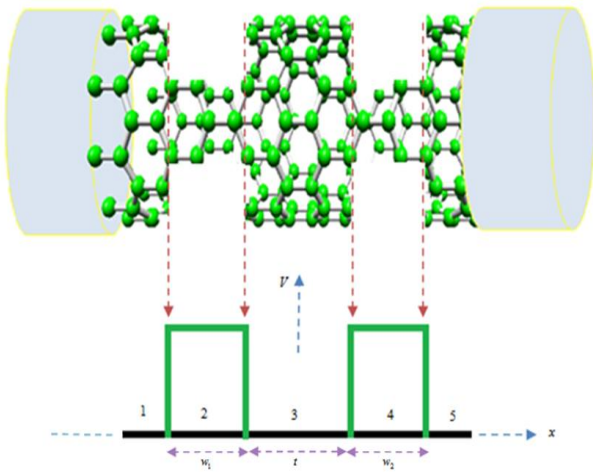


Figure (4): Multi-barrier channel region in GNS transistor Hence, to deducing the innovative T (E), assume that solutions to Schrodinger's equation through in every district for $E < V_0$:

$$\begin{aligned}\psi_1(x) &= Ae^{ik_1x} + Be^{-ik_1x}, x < a \\ \psi_2(x) &= Ce^{k_2x} + De^{-k_2x}, a < x < b \\ \psi_3(x) &= Fe^{ik_3x} + Ge^{-ik_3x}, b < x < c \\ \psi_4(x) &= He^{k_4x} + Je^{-k_4x}, c < x < d \\ \psi_5(x) &= Ke^{ik_5x} + Le^{-ik_5x}, d < x\end{aligned}\quad (4)$$

Someplace $(k_1 = k_3 = k_5 = k)$ and $(k_2 = k_4 = K)$ have their usual forms as certain in equation (2) and the locations of the interfaces have been labeled a, b, c and d, correspondingly. Normal Ben Daniel-Duke [42] boundary conditions at every crossing point gives the following

$$\begin{cases} \psi_1(x)|_{x=0} = \psi_2(x)|_{x=0} \rightarrow A + B = C + D \\ \frac{d\psi_1(x)}{dx}|_{x=0} = \frac{d\psi_2(x)}{dx}|_{x=0} \rightarrow ik_1A - ik_1B = k_2C - k_2D \end{cases}$$

$$\begin{cases} \psi_2(x)|_{x=b} = \psi_3(x)|_{x=b} \rightarrow Ce^{k_2b} + De^{-k_2b} = Fe^{ik_3b} + Ge^{-ik_3b} \\ \frac{d\psi_2(x)}{dx}|_{x=b} = \frac{d\psi_3(x)}{dx}|_{x=b} \rightarrow Ck_2e^{k_2b} - Dk_2e^{-k_2b} = ik_3Fe^{ik_3b} - ik_3Ge^{-ik_3b} \end{cases}$$

$$\begin{cases} \psi_3(x)|_{x=c} = \psi_4(x)|_{x=c} \rightarrow Fe^{ik_3c} + Ge^{-ik_3c} = He^{k_4c} + Je^{-k_4c} \\ \frac{d\psi_3(x)}{dx}|_{x=c} = \frac{d\psi_4(x)}{dx}|_{x=c} \rightarrow ik_3Fe^{ik_3c} - ik_3Ge^{-ik_3c} = Hk_4e^{k_4c} - Jk_4e^{-k_4c} \end{cases}\quad (5)$$

$$\begin{cases} \psi_4(x)|_{x=d} = \psi_5(x)|_{x=d} \rightarrow He^{k_4d} + Je^{-k_4d} = Ke^{ik_5d} \\ \frac{d\psi_4(x)}{dx}|_{x=d} = \frac{d\psi_5(x)}{dx}|_{x=d} \rightarrow Hk_4e^{k_4d} - Jk_4e^{-k_4d} = ik_5Ke^{ik_5d} \end{cases}$$

The solving method is to transport matrix technique as previous; the derived equation indicates the matrix form of the model.

$$\begin{pmatrix} 1 & 1 \\ ik_1 & -ik_1 \end{pmatrix} \begin{pmatrix} A \\ B \end{pmatrix} = \begin{pmatrix} 1 & 1 \\ k_2 & -k_2 \end{pmatrix} \begin{pmatrix} C \\ D \end{pmatrix} \rightarrow M_1 \begin{pmatrix} A \\ B \end{pmatrix} = M_2 \begin{pmatrix} C \\ D \end{pmatrix}$$

$$\begin{aligned} \begin{pmatrix} e^{k_2b} & e^{-k_2b} \\ k_2e^{k_2b} & -k_2e^{-k_2b} \end{pmatrix} \begin{pmatrix} C \\ D \end{pmatrix} &= \begin{pmatrix} e^{ik_3b} & e^{-ik_3b} \\ ik_3e^{ik_3b} & -ik_3e^{-ik_3b} \end{pmatrix} \begin{pmatrix} F \\ G \end{pmatrix} \rightarrow M_3 \begin{pmatrix} C \\ D \end{pmatrix} = M_4 \begin{pmatrix} F \\ G \end{pmatrix} \\ \begin{pmatrix} e^{ik_3c} & e^{-ik_3c} \\ ik_3e^{ik_3c} & -ik_3e^{-ik_3c} \end{pmatrix} \begin{pmatrix} F \\ G \end{pmatrix} &= \begin{pmatrix} e^{k_4c} & e^{-k_4c} \\ k_4e^{k_4c} & -k_4e^{-k_4c} \end{pmatrix} \begin{pmatrix} H \\ J \end{pmatrix} \rightarrow M_5 \begin{pmatrix} F \\ G \end{pmatrix} = M_6 \begin{pmatrix} H \\ J \end{pmatrix} \\ \begin{pmatrix} e^{k_4d} & e^{-k_4d} \\ k_4e^{k_4d} & -k_4e^{-k_4d} \end{pmatrix} \begin{pmatrix} H \\ J \end{pmatrix} &= \begin{pmatrix} e^{ik_5d} & 0 \\ ik_5e^{ik_5d} & 0 \end{pmatrix} \begin{pmatrix} K \\ L \end{pmatrix} \rightarrow M_7 \begin{pmatrix} H \\ J \end{pmatrix} = M_8 \begin{pmatrix} K \\ L \end{pmatrix} \end{aligned}\quad (6)$$

Then, as before, outer regions coefficients of the can be linked by forming the transfer matrix,

$$\begin{pmatrix} A \\ B \end{pmatrix} = M_1^{-1}M_2M_3^{-1}M_4M_5^{-1}M_6M_7^{-1}M_8 \begin{pmatrix} K \\ L \end{pmatrix}$$

$$M_1^{-1} = \frac{1}{-2ik_1} \begin{pmatrix} -ik_1 & -1 \\ -ik_1 & 1 \end{pmatrix}, M_3^{-1} = \frac{1}{-2k_2} \begin{pmatrix} -k_2e^{-k_2b} & -e^{-k_2b} \\ -k_2e^{k_2b} & e^{k_2b} \end{pmatrix}$$

$$M_5^{-1} = \frac{1}{-2ik_3} \begin{pmatrix} -ik_3e^{-ik_3c} & -e^{-ik_3c} \\ -ik_3e^{ik_3c} & e^{ik_3c} \end{pmatrix}, M_7^{-1} = \frac{1}{-2k_4} \begin{pmatrix} -k_4e^{-k_4d} & -e^{-k_4d} \\ -k_4e^{k_4d} & e^{k_4d} \end{pmatrix}\quad (7)$$

$$\begin{pmatrix} A \\ B \end{pmatrix} = \frac{1}{-16k_1k_2k_3k_4} \begin{pmatrix} -ik_1 & -1 \\ -ik_1 & 1 \end{pmatrix} \begin{pmatrix} 1 & 1 \\ k_2 & -k_2 \end{pmatrix} \begin{pmatrix} -k_2e^{-k_2b} & -e^{-k_2b} \\ -k_2e^{k_2b} & e^{k_2b} \end{pmatrix} \begin{pmatrix} e^{ik_3b} & e^{-ik_3b} \\ ik_3e^{ik_3b} & -ik_3e^{-ik_3b} \end{pmatrix} \\ * \begin{pmatrix} -ik_3e^{-ik_3c} & -e^{-ik_3c} \\ -ik_3e^{ik_3c} & e^{ik_3c} \end{pmatrix} \begin{pmatrix} e^{k_4c} & e^{-k_4c} \\ k_4e^{k_4c} & -k_4e^{-k_4c} \end{pmatrix} \begin{pmatrix} -k_4e^{-k_4d} & -e^{-k_4d} \\ -k_4e^{k_4d} & e^{k_4d} \end{pmatrix} \begin{pmatrix} e^{ik_5d} & 0 \\ ik_5e^{ik_5d} & 0 \end{pmatrix} \begin{pmatrix} K \\ L \end{pmatrix}\quad (8)$$

Indeed, apparently, this is a 2×2 matrix equation with four unknown parameters and cannot be resolved at this stage.

Previously, the standard limits, that is $\psi_z \rightarrow 0$, as $z \rightarrow \pm\infty$ is used. Some states within the quantum wells is not suitable to find the wave form including traveling waves in the barrier structures therefore the 2×2 matrix can be written as M, then:

$$\begin{pmatrix} A \\ B \end{pmatrix} = M \begin{pmatrix} K \\ L \end{pmatrix} \rightarrow A = M_{11}K\quad (9)$$

The transmission coefficient is:

$$T(E) = \frac{K^*K}{A^*A} = \frac{1}{M_{11}^*M_{11}}\quad (10)$$

We impellent scaled-down version of the double-barrier position; transfer income formula amplitude is written as:

$$t(E) = 4 \left[e^{ik_1(w_1+w_2)} (2 \cosh(k_3w_2) - ik_{1-3} \sinh(k_3w_2)) (2 \cosh(k_2w_1)) - ik_{1-2} \sinh(k_2w_1) + e^{ik_1(g+b-w_1)} k_{1+3} k_{1+2} \sinh(k_2w_1) \sinh(k_3w_2) \right]^{-1}\quad (11)$$

Therefore $w_{1,2}$ represents widths of the two barriers and t is the distance between the barrier and Additional parameters are

$$g = w_1 + w_2, b = w_1 + w_2 + t, k_{i\pm j} = \frac{k_i}{k_j} \pm \frac{k_j}{k_i}, (i, j = 1, 2, 3)$$

as a result:

$$t(E) = \frac{4ik_1^2k_2^2e^{-2mw_1}}{\left((-ik_1^4 - 2ik_1^2k_2^2 - ik_2^4)e^{2i(t-w_1)k_1} + ik_1^4 - 2ik_1^2k_2^2 + ik_2^4 + (ik_1^4 + 2ik_1^2k_2^2 + ik_2^4)e^{2i(t-w_1)k_1} \cosh^2(w_1k_2) \right) \left((-ik_1^4 + 6ik_1^2k_2^2 - ik_2^4) \cosh^2(w_1k_2) + 4k_1k_2(k_1^2 - k_2^2) \sinh(w_1k_2) \cosh(w_1k_2) \right)} \quad (12)$$

Therefore the transmission coefficient is a guess of how a large deal of an electromagnetic wave (light) exceed throughout an outside or an optical constituent. Transmission coefficients are able to affects amplitude or the intensity of the wave as well is intended by gorgeous relation of the assessment subsequent to the outside or constituent to the worth. This complete square provides the transmission coefficient T. Therefore the transmission coefficient is calculated as

$$T(E) = \frac{16k_1^2k_2^2}{\left((k_1^4 + 2k_1^2k_2^2 + k_2^4) \sin(2k_1(t-w_1)) - (k_1^4 + 2k_1^2k_2^2 + k_2^4) \sin(2k_1(t-w_1)) \cosh^2(w_1k_2) \right)^2 + 4 \sinh(w_1k_2) k_1k_2(k_1^2 - k_2^2) \cosh(w_1k_2) + \left(-\cos(2k_1(t-w_1)) (k_1^4 + 2k_1^2k_2^2 + k_2^4) + k_1^4 - 2k_1^2k_2^2 + k_2^4 + (\cos(2k_1(t-w_1)) (k_1^4 + 2k_1^2k_2^2 + k_2^4) - k_1^4 + 6k_1^2k_2^2 - k_2^4) \cosh^2(w_1k_2) \right)^2} \quad (13)$$

In foregoing equation, the wave vector ($k_1 = k$) outside the barrier is a real quantity for all positive energies E of the electron. The minimum conduction band in the region outside barrier taken as zero energy. Since the minimum conduction band of barrier is above that of the region outside and hence as for certain energies of the electron ($E < V_0$) the wave vector ($k_2 = K$) will be imaginary and for energies above V_0 ($E > V_0$) is real. Thus the energy can be divided into two regions, ($E < V_0$) for non-classical transition through tunneling and ($E > V_0$) where transition can occurs even under classical conditions.

The solutions and methods applied to evaluate the transmission coefficients in the two regions will be differed among many others. Since ($k_1 = k$) and ($k_2 = K$) are both effective mass and energy-dependent, hence for different material pairs the variation of the transmission coefficient for energy values is normalized with given barriers height [39, 40,41]. Where w_1, w_2 are the lengths of the barriers.

The transmission coefficient of electrons through a potential barrier is important for studying the leakage current in MOSFETs with nanometer dimensions. It is at the same time a crucial parameter to shed lights on behavior of multiple quantum well structures where the barriers are sandwiched between two coupled quantum wells. When the wells and barriers regions are in the nanometer range we expect further

quantization of the energy levels. This is being considered in a further study of the multiple quantum well structure. The less barriers width, the more tunneling and transmission coefficient value with normalized electron energy will be

more. For $\left(E_n = \frac{E}{V_0} \right) < 1$, the transmission coefficient increases from 0 to 1 in a non-linear manner as figure (5, 6) illustrates it.

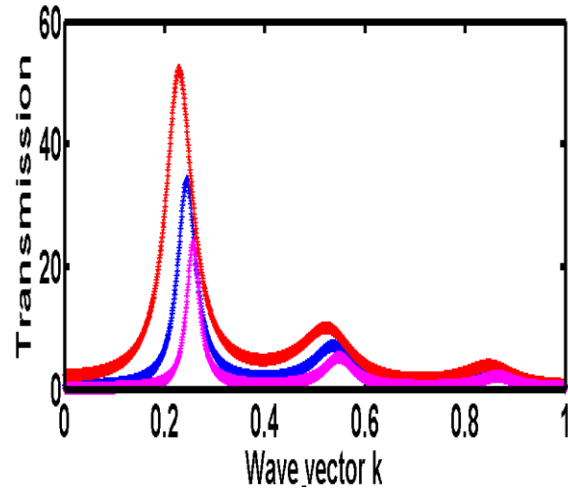


Figure (5): Transmission for different K (0.8(violet), 0.7(blue), 0.6(red)) values in the GNS at Chanel region

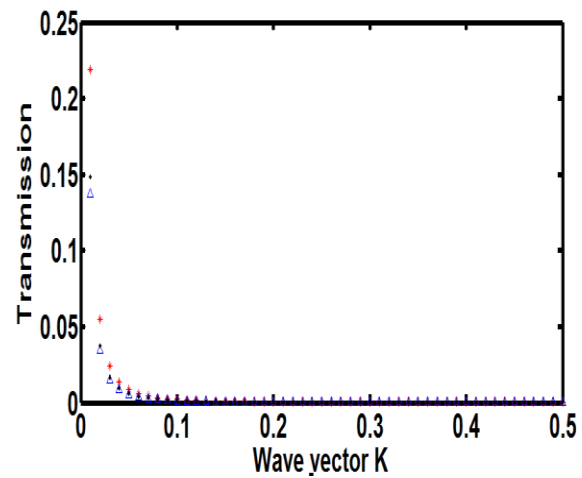


Figure (6): Transmission for different k (0.8(black), 0.7(blue), 0.6(red)) values in the GNS_ at first, third and the fifth regions

As shown in figure (5) and figure (6) if the energy of electron in each region is changed within allowed values the transmission coefficient is varied accordingly.

Figure (7) in addition gives an example of the Transmission coefficient for barriers with height V as a function for different t (t=1.5(blue), 2.5(red), 3.5(black)) of the distance t between them. Also figure (8) show the Transmission coefficient for barriers with height V as a function for different w_1 ($w_1=0.5$ (blue),1.0(red),1.5(black))

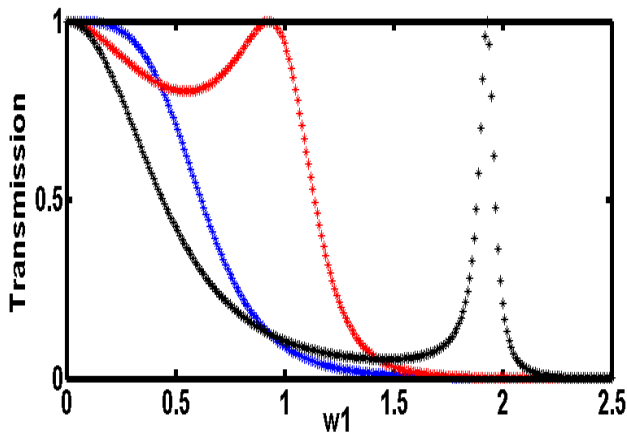


Figure (7): Transmission for different t (t=1.5(blue), 2.5(red), 3.5(black)) values in the GNS at third region

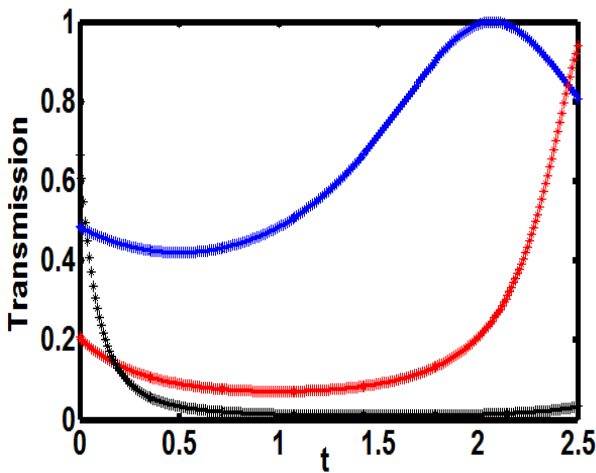


Figure (8): Transmission for different w_1 ($w_1=0.5$ (blue), 1.0 (red), 1.5 (black)) values in the GNS at third regions

As expected it is indeed apparent that results from the resonance increases transmission which classically suggests a reduction on the transmission ratio that means it is more difficult for electrons to tunnel through barriers. Increasing the resonance energy by applied voltage will increase effect of confinement barrier height and high-energy resonance appearance, manifesting quasi-bound state [show me the reference]. In fact, the features, including two-terminal electronic devices as a whole it can be summarized with their current-voltage characteristics (I-V). In simplified form given wave vector and quantum transmission coefficient the quantum current will be modified as

$$T(E) = \frac{16\alpha(1 - \frac{E_g}{E})}{\left(\left(1 + 2\alpha(1 - \frac{E_g}{E}) + \alpha^2(1 - \frac{E_g}{E})^2 \right) \sin(2\beta\sqrt{E}(t-w_1)) - \left(1 + 2\alpha(1 - \frac{E_g}{E}) + \alpha^2(1 - \frac{E_g}{E})^2 \right) \sin(2\beta\sqrt{E}(t-w_1)) \cosh^2(\gamma\sqrt{E-E_g}) \right)^2 + 4\left(\alpha(1 - \frac{E_g}{E})(1 - \alpha + \frac{E_g}{E}) \sinh(\gamma\sqrt{E-E_g}) \cosh(\gamma\sqrt{E-E_g}) \right)^2 } + \frac{\left(-1 + 2\alpha(1 - \frac{E_g}{E}) + \alpha^2(1 - \frac{E_g}{E})^2 \right) \cos(2\beta\sqrt{E}(t-w_1)) + \left(1 - 2\alpha(1 - \frac{E_g}{E}) + \alpha^2(1 - \frac{E_g}{E})^2 \right) + \left(1 + 2\alpha(1 - \frac{E_g}{E}) + \alpha^2(1 - \frac{E_g}{E})^2 \right) \cos(2\beta\sqrt{E}(t-w_1)) \cosh^2(\gamma\sqrt{E-E_g}) - \left(1 - 6\alpha(1 - \frac{E_g}{E}) + \alpha^2(1 - \frac{E_g}{E})^2 \right) \cosh^2(\gamma\sqrt{E-E_g}) }{2} \quad (14)$$

Where

$$\beta = \sqrt{\frac{2m}{\hbar^2}}, \alpha = \frac{\hbar^2}{3tma_{cc}}, \gamma = \sqrt{\frac{2}{3ta_{cc}}}, k_1 = \beta\sqrt{E}, k_2 = \gamma\sqrt{E-E_g}$$

Also Figure (9) gives an example of the Transmission coefficient for barriers of height as a function of the distance t between them.

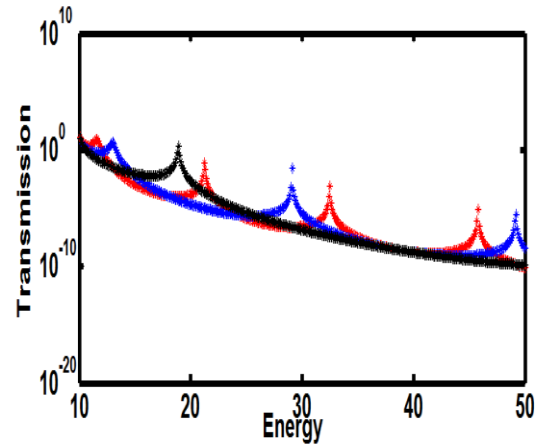


Figure (9): Transmission coefficient as a function of the energy through a double barrier of height, separated by a distance t

It is obvious that the results from the resonance increase the transmission T as expected which classically indicates a reduction on the transmission ratio that means it is more difficult for electrons to tunnel through the barriers. Increasing the resonance energy by applied voltage will increase the effect of confinement barrier height and appearance of the high-energy resonance is a reflection of the quasi-bound state existence [show me the reference]. In fact, the features, such as two-terminal electronic devices in general can be summarized with their current-voltage characteristics (I-V).

III. CONCLUSION

Additionally, structural parameter effect on quantum current of graphene based transistor is analyzed. Finally, At low temperatures, a small part of the energy carriers in the space around the band minima. Since the area has increased, the current starts flowing only when this narrow resonance line with the distribution of energy, and thus Current peak is narrow. When the temperature rises, the carrier distribution is expanding, so that it is more the range of applied voltage, which is a degree of alignment of the resonance energy carrier. The peak occurs when

The distribution corresponds to the peak of the resonance energy. At voltages above this, the number of carriers available Reducing the tunnel and thus reduce the power.

Also in this paper, transmission coefficient increases with increasing K and thus transmission coefficient peak is narrow.

IV.ACKNOWLEDGMENT

Authors would like to acknowledge the financial support from Research University grant of the Uremia University. Also thanks to the Research Management Center of Uremia University for providing excellent research environment in which to complete this work.

REFERENCES

- [1] Geim AK, Novoselov KS: The rise of graphene. *Nat Mater* 2007, 6: 183–191. 10.1038/nmat1849 View Article Google Scholar
- [2] Geim AK: Graphene: status and prospects. *Science* 2009, 324: 1530–1534. 10.1126/science.1158877 View Article Google Scholar
- [3] Shi X, Pugno NM, Gao H: Mechanics of carbon nanoscrolls: a review. *Acta Mechanica Sinica* 2010, 23(6):484–497. 10.1016/S0894-9166(11)60002-5 View Article Google Scholar
- [4] Mpourmpakis G, Tylianakis E, Froudakis GE: Carbon nanoscrolls: a promising material for hydrogen storage. *Nanoletters* 2007, 7(7):1893–1897. 10.1021/nl070530u View Article Google Scholar
- [5] Zeng F, Kuang Y, Liu G, Liu R, Huang Z, Fuab C, Zhou H: Supercapacitors based on high-quality graphene scrolls. *Nanoscale* 2012, 4: 3997–4001. 10.1039/c2nr30779k View Article Google Scholar
- [6] M. Grundmann, "Nan scroll formation from strained layer heterostructures," *Applied Physics Letters*, vol. 83, no. 12, pp. 2444–2446, 2003. View at Publisher · View at Google Scholar · View at Scopus
- [7] S. F. Braga, V. R. Coluci, S. B. Legoas, R. Giro, D. S. Galvão, and R. H. Baughman, "Structure and dynamics of carbon nanoscrolls," *Nano Letters*, vol. 4, no. 5, pp. 881–884, 2004. View at Publisher · View at Google Scholar · View at Scopus
- [8] B. V. C. Martins and D. S. Galvão, "Curved graphene nanoribbons: structure and dynamics of carbon nanobelts," *Nanotechnology*, vol. 21, no. 7, Article ID 075710, 2010. View at Publisher · View at Google Scholar
- [9] Y. Chen, J. Lu, and Z. Gao, "Structural and electronic study of nanoscrolls rolled up by a single graphene sheet," *Journal of Physical Chemistry C*, vol. 111, no. 4, pp. 1625–1630, 2007. View at Publisher · View at Google Scholar · View at Scopus
- [10] X. Peng, J. Zhou, W. Wang, and D. Cao, "Computer simulation for storage of methane and capture of carbon dioxide in carbon nanoscrolls by expansion of interlayer spacing," *Carbon*, vol. 48, no. 13, pp. 3760–3768, 2010. View at Publisher · View at Google Scholar · View at Scopus
- [11] A. K. Schaper, H. Hou, M. Wang, Y. Bando, and D. Goldberg, "Observations of the electrical behavior of catalytically grown scrolled graphene," *Carbon*, vol. 49, no. 6, pp. 1821–1828, 2011. View at Publisher · View at Google Scholar · View at Scopus
- [12] X. Xie, L. Ju, X. Feng et al., "Controlled fabrication of high-quality carbon nanoscrolls from monolayer graphene," *Nano Letters*, vol. 9, no. 7, pp. 2565–2570, 2009. View at Publisher · View at Google Scholar · View at Scopus
- [13] G. Xi, M. Zhang, D. Ma, Y. Zhu, H. Zhang, and Y. Qian, "Controlled synthesis of carbon nanocables and branched-nanobelts," *Carbon*, vol. 44, no. 4, pp. 734–741, 2006. View at Publisher · View at Google Scholar · View at Scopus
- [14] Y.-X. Qi, M.-S. Li, and Y.-J. Bai, "Carbon nanobelts synthesized via chemical metathesis route," *Materials Letters*, vol. 61, no. 4-5, pp. 1122–1124, 2007. View at Publisher · View at Google Scholar · View at Scopus
- [15] X. Shi, N. M. Pugno, and H. Gao, "Mechanics of carbon nanoscrolls: a review," *ActaMechanicaSinica*, vol. 23, no. 6, pp. 484–497, 2010. View at Publisher · View at Google Scholar · View at Scopus
- [16] K. S. Kim, Y. Zhao, H. Jang et al., "Large-scale pattern growth of graphene films for stretchable transparent electrodes," *Nature*, vol. 457, no. 7230, pp. 706–710, 2009. View at Publisher · View at Google Scholar · View at Scopus
- [17] G. Mpourmpakis, E. Tylianakis, and G. E. Froudakis, "Carbon nanoscrolls: a promising material for hydrogen storage," *Nano Letters*, vol. 7, no. 7, pp. 1893–1897, 2007. View at Publisher · View at Google Scholar · View at Scopus
- [18] E. Perim and D. S. Galvao, "The structure and dynamics of boron nitride nanoscrolls," *Nanotechnology*, vol. 20, no. 33, Article ID 335702, 2009. View at Publisher · View at Google Scholar · View at Scopus
- [19] A. Cao, G. Meng, and P. M. Ajayan, "Nanobelt-templated growth of carbon nanotube rows," *Advanced Materials*, vol. 16, no. 1, pp. 40–44, 2004. View at Publisher · View at Google Scholar · View at Scopus
- [20] L. H. Viculis, J. J. Mack, and R. B. Kaner, "A chemical route to carbon nanoscrolls," *Science*, vol. 299, no. 5611, p. 1361, 2003. View at Publisher · View at Google Scholar · View at Scopus
- [21] D. Xia, J. Xie, H. Chen et al., "Fabrication of carbon nanoscrolls from monolayer graphene," *Small*, vol. 6, no. 18, pp. 2010–2019, 2010. View at Publisher · View at Google Scholar · View at Scopus
- [22] Braga,S.F., Coluci,V.R., Legoas,S.B., Giro,R., Galvao,D.S. and Baughman,R.H., Structure and dynamics of carbon nanoscrolls. *Nano Letters*, 2004, 4: 881-884.
- [23] Shi,X.H., Pugno,N.M. and Gao,H.J., Tunable core size of carbon nanoscrolls. *Journal of Computational and Theoretical Nanoscience*, 2010, 7: 517-521.
- [24] S. Datta, *Quantum Transport: Atom to Transistor*, Cambridge University Press, Cambridge. (2005)
- [25] M. T. Ahmadi and J. F. Webb, *Carbon-Based Materials Concepts and Basic Physics* 49 (2012).
- [26] Zeng, F., et al., Facile Preparation of High - Quality Graphene Scrolls from Graphite Oxide by a Microexplosion Method. *Advanced Materials*, 2011. 23(42): p. 4929-4932.
- [27] Martins, B.V.C.and D.S.Galvao, Curved graphene nanoribbons: structure and dynamics of carbon nanobelts. *Nanotechnology*, 2010. 21(7).
- [28] Xie, X., et al., Controlled Fabrication of High - Quality Carbon Nanoscrolls from Monolayer Graphene. *Nano Letters*, 2009. 9(7): p. 2565 - 2570.
- [29] Lima, M.D., et al., Biscrolling Nanotube Sheets and Functional Guests into Yarns. *Science*, 2011. 331(6013): p. 51- 55.
- [30] Zhu, S.and T. Li, Hydrogenation enabled scrolling of graphene. *Journal of Physics D - Applied Physics*, 2013. 46(7).
- [31] Shi, X.H., et al., A translational nanoactuator based on carbon nanoscrolls on substrates. *Applied Physics Letters*, 2010. 96(5).
- [32] Roy, D., et al., Synthesis and Raman spectroscopic characterisation of carbon nanoscrolls. *Chemical Physics Letters*, 2008. 465(4-6): p. 254-257.
- [33] Li, T.S., et al., Quantum transport in carbon nanoscrolls. *Physics Letters A*, 2012. 376(4): p. 515-520
- [34] Bai, J., et al., Graphene nanomesh. *Nature Nanotechnology*, 2010. 5(3): p. 190 - 194.
- [35] Anderson, B.A.and E.J. Nowak, Graphene-based field effect transistor has pair of graphene layers located on pair of sidewalls of silicon carbide fin, 2009, Anderson B a; Nowak E J.
- [36] Berger, C., et al., Ultrathin epitaxial graphite: 2D electron gas properties and a route toward graphene-based nanoelectronics. *Journal of Physical Chemistry B*, 2004. 108: p. 19912-19916.
- [37] Akhmerov, A.R., et al., Theory of the valley-valve effect in graphene nanoribbons. *Physical Review B*, 2008. 77(20).
- [38] Enoki, T., Y. Kobayashi, and K. -I. Fukui, Electronic structures of graphene edges
- [39] Chen,Y., Lu,J. and Gao,Z.X., Structural and electronic study of nanoscrolls rolled up by a single graphene sheet. *The Journal of Physical Chemistry C*, 2007, 111: 1625-1630.
- [40] Shi,X.H.,Pugno,N.M., Cheng,Y., and Gao,H.J., "Gigahertz breathing oscillators based on carbon nanoscrolls. " *APPLIED PHYSICS LETTERS* 95, 163113 2009.
- [41] H.Karimi, M.Ahmadi, E.Khosrowabadi,R.Rahmani, M.Saeidimanesh, R.Ismail,S.D.Naghieb and E.Akbari.(2014) , " Analytical prediction of liquid-gated graphene nanoscroll biosensor performance"The

Royal Society of Chemistry, 4,16153–16162.

[42] Pan, H., et al. (2005). "Ab initio study of electronic and optical properties of multiwall carbon nanotube structures made up of a single rolled-up graphite sheet." *Physical Review B* 72(8).

[43] Lee, J. U., et al. (2004). "Carbon nanotube p-n junction dodes." *Applied Physics Letters* 85(1): 145.

[44] Khaledian, M., et al. (2014). "Structural and Properties of Graphene Nanobelts Rolled Up Into Spiral by a Single Graphene Sheet." *Journal of Computational and Theoretical Nanoscience* 11(3): 601-606.
